EEG sensor system development consisting of solid polyvinyl alcohol−glycerol−NaCl contact gel and 3D-printed, silver-coated polylactic acid electrode for potential brain−computer interface use

K. Jakab [a, b], J. Csipor [c], I. Ulbert [c, d], Z. Keresztes [a], G. Mészáros [a, *], G. Márton [c, d]

[a] Research Centre for Natural Sciences, Institute of Materials and Environmental Chemistry, Functional Interfaces Research Group, Magyar Tudósok krt. 2, H-1117, Budapest, Hungary
[b] Budapest University of Technology and Economics, Faculty of Chemical Technology and Biotechnology Department of Inorganic and Analytical Chemistry, Hungary
[c] Research Centre for Natural Sciences, Institute of Cognitive Neuroscience and Psychology, Integrative Neuroscience Research Group, Magyar Tudósok krt. 2, H-1117, Budapest, Hungary
[d] Faculty of Information Technology and Bionics, Pázmány Péter Catholic University, Hungary

ARTICLE INFO

ABSTRACT

The paper describes the development of a reusable electrode system for non-invasive brain−computer interface application with signal quality comparable to that of conventional wet Ag/AgCl electrodes. The innovative electrode system consists of a polyvinyl alcohol−glycerol−NaCl contact hydrogel and a 3D-printed, silver-coated polylactic acid electrode body. Advantageous features of the proposed system are the comfortable use, reusability, long shelf life, and alterable geometry. The electrical properties of freshly prepared and aged contact gels, as well as different gel/silver interfaces, were separately characterized, showing much lower impedance values than those measured at the electrode−skin interface with the complete electrode system. Acceptability limits relevant to electroencephalographic measurements, such as signal-to-noise ratio during steady-state visually evoked potential measurements and band ratio values during alpha wave detection, have proven the applicability of the system.
© 2022 The Author(s). Published by Elsevier Ltd. This is an open access article under the CC BY-NC-ND license (http://creativecommons.org/licenses/by-nc-nd/4.0/).

1. Introduction

Electroencephalography (EEG) is a well-known method for electrical brain signal acquisition. The popularity of EEG is due to its non-invasive nature and the achievable high temporal resolution. EEG is used for such medical diagnoses for evaluating sleep disorders, stroke, epilepsy, and brain death. EEG is also most commonly used for brain−computer interface (BCI) applications due to its advantages compared to other invasive methods. The fact that there is no need for a surgery makes involving participants easier, conducting experiments more convenient and safer. It is also possible to study a larger volume of the brain with this approach. A BCI is a computer-based system that translates captured brain signals into commands in real time. BCIs have been gaining popularity in the past decade; they are primarily used in medicine to aid paralyzed patients to regain communication toward and control over their locomotive system. Recently, human lifestyle enhancement applications have also appeared [1,2].

For electroencephalographic signal acquisition, conventional wet Ag/AgCl electrodes have been used almost exclusively for a long time and are also considered to be the golden standard. They provide sufficiently low electrode−skin impedance and good signal quality. However, wet electrodes possess three main disadvantages. First, the placement of the electrodes on the scalp is a lengthy process that should be carried out by an expert. Second, the conductive gel or paste applied as electrode−skin interface often causes discomfort to the patient, since it can irritate and damage the scalp, and the removal of this substance from the hair after recording also comes with inconvenience. Finally, due to dehydration, long-term measurement is only feasible if the gel is reapplied to the electrode surfaces. Solid hydrogels absorbing conductive solutions are not regarded as conductive gels in this paper.

To overcome the drawbacks of the conventional wet EEG electrodes, several dry sensor designs have been proposed; these electrodes do not require the application of electrolytes or

* Corresponding author.
E-mail address: meszaros.gabor@ttk.hu (G. Mészáros).

conductive gels; however, a small amount is usually still present at the electrode−skin interface due to adsorbed sweat and moisture. Popular are the microneedle electrode arrays produced by micro-machining silicon wafers. The needles are usually shaped as pillars, cones, or pyramids. These arrays also must be coated with some conductive materials such as metals (Au, Ag) or metal oxides (IrO). The main advantage of these sensors is that they bypass the skin's outer layer, the *stratum corneum*, thus greatly lowering the electrode−skin impedance. However, the brittle needles may break causing infections, and they can only be used on non-hairy sites due to their shortness [3−5]. Similar results have been attained by the preparation of a carbon nanotube array sensor [6]. Pin-shaped polymer sensors are also favored as an electrode design. Their base materials include rigid and flexible polymers as well, such as polylactic acid (PLA), polyamides, thermoplastic polyurethane, rubber and acrylonitrile butadiene styrene . Most of these can be 3D printed, thus granting a great freedom in electrode geometry. The polymer must contain or has to be coated with a conductive component, such as gold, silver, carbon or carbon nanotube, poly(3,4-ethylenedioxythiophene), and so on [7−12], with similar strategy as polymer-based nanocomposite electrodes are used in analytical assays [13−15]. Several unique electrode designs have also been mentioned in the recent literature: sensor made of silver-coated polymer bristles [16], electrically conductive foam covered by a conductive fabric [17] and a sensor that uses gold-coated spring contact probes for low impedance signal acquisition [18]. A flexible Ag/AgCl electrode array was also developed, which lowers the contact impedance by using a sweat-absorbing sponge during forehead recordings [19].

Semi-dry electrode designs have been proposed in the past decade combining the advantages of wet and dry electrodes while alleviating their drawbacks. The semi-dry sensors wet the scalp via the use of minimal amounts of electrolytes providing lower impedance at the electrode−skin interface than in the case of dry sensors while preventing short circuits and staining the subject's hair. The electrolyte seepage of electrodes can be realized by active pressure or passively via capillary force or gravity, realized either by possessing reservoirs that leak the conductive liquid or by the use of porous materials such as hydrogels. Design with reservoirs was first used by Mota et al. [20] where they developed an Ag/AgCl-coated flexible polyurethane electrode with a cavity for the electrolyte. This was later adapted to make semi-dry electrodes using porous Ti and a micro-seepage sponge-based electrode design [21,22]. Solid hydrogels were also employed as semi-dry electrodes to enable gradual scalp wetting; these include carboxymethylcellulose [23], alginate [24], polyacrylate [25] and polyvinyl alcohol [26]. The latest development in the field of semi-dry electrode has been made by Pedrosa et al. [27] and Li et al. [28], where they designed electrode systems capable of controlled fluid release through capillary force via porous polycarbonate or ceramic wicks. A similar construction was also made with the use of a poly-acrylamide/polyvinyl alcohol composite gel yielding a sensor that can "charge−discharge" electrolyte like a battery [26].

PVA hydrogels have been used in biomedical applications and recently as a flexible conductor material [29−31]. The gelation of PVA can be done chemically or physically. In the case of the former, small crosslinker molecules, like glutaraldehyde or another macro-molecule, such as alginate or gelatine are needed [32−34]. The most common way of physical PVA crosslinking is the freezing-thawing method, during which gels with excellent elasticity can be obtained thanks to microcrystal formation. The properties of such hydrogels were thoroughly investigated by N. Peppas and C. Hassan
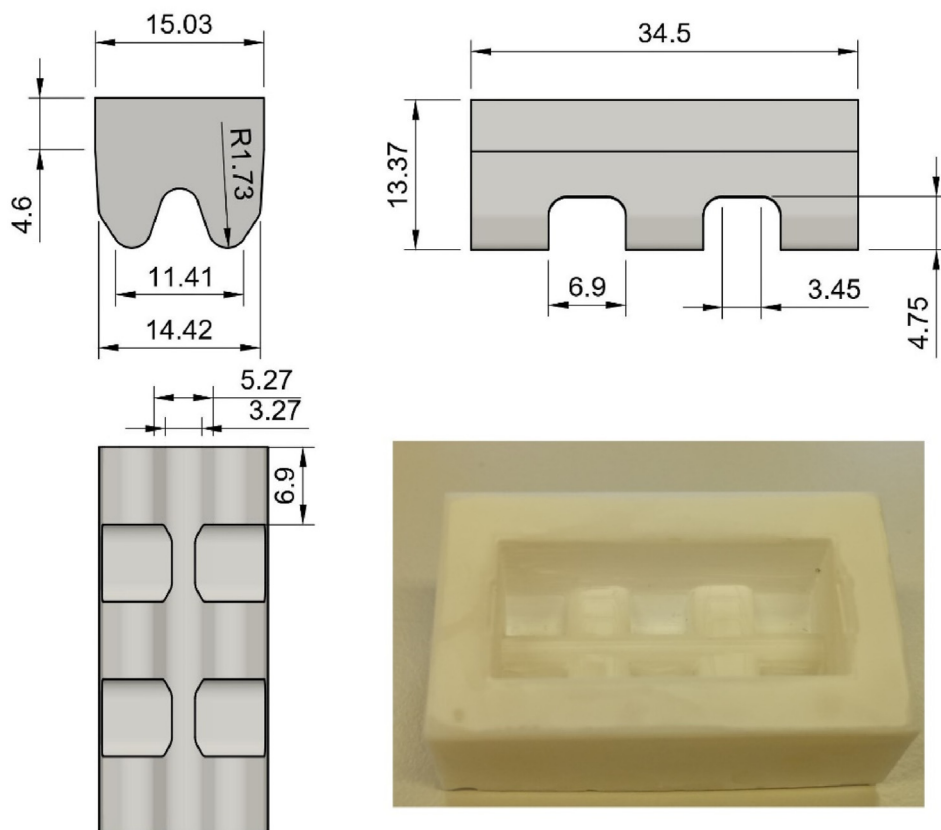

Fig. 1. The negative of the molds used for the electrode production and the printed mold (bottom right). All length values depicted are in millimeter unit.
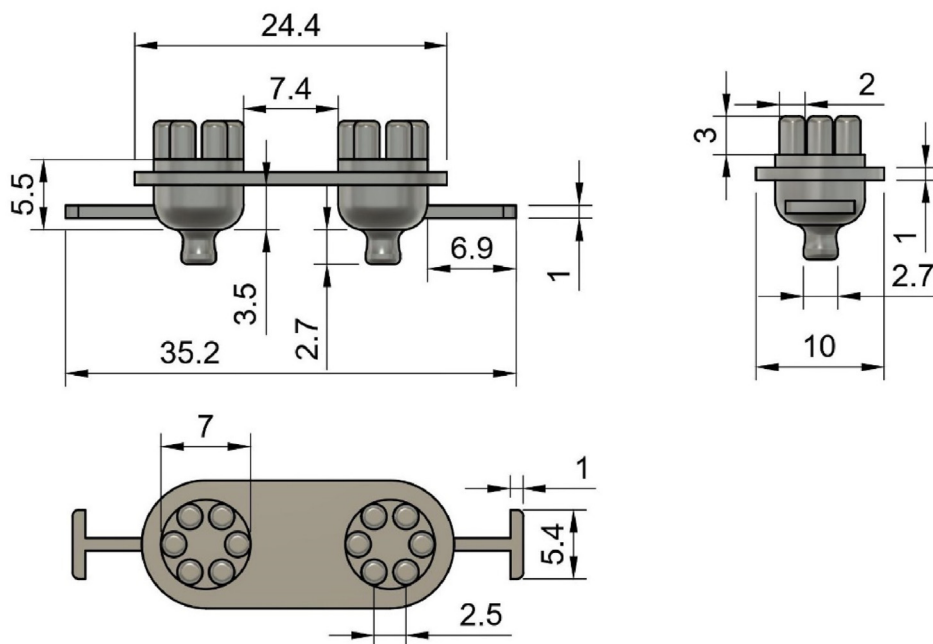
Fig. 2. Design of the PLA electrode bodies. The snap connectors and the positioning arms on the side are to be noted. All length values depicted are in millimeter unit.

[35−39]. The modification of the original method is being explored extensively in the literature [40−43]. Recently, Shi et al. [44] used a water−glycerol mixture as a base for the polymer solution achieving excellent mechanical properties and gelation at room temperature, due to the physical, hydrogen-bond-mediated crosslinks.

Our aim was to integrate the low impedance of solid gel based and the long-term usability of dry EEG electrodes by gel structure modification. We have used a modified Peng et al.'s [29,45] method of PVA gelation for our electrode design. The produced polyvinyl alcohol−glycerol−NaCl hydrogels (PVA gel) possess high ionic conductivity that enables good signal transfer; their glycerol content provides longer shelf life, since it inhibits dehydration and prevents mold formation. The solidity and flexibility ensure that the gel follows the shape of the skull for better contact and that only minimal liquid residue remains on the scalp. Furthermore, a wide range of geometrical configurations are available due to the gel casting manufacturing method, which enables brain signal detection on hairy sites. 3D-printed PLA bodies (AgPLA) were used as the interface between the solid gel and the electrical wiring to convert ionic to electric current. The AgPLA bodies were coated with silver paint to provide conductive properties [9]. The solid gel, the silver−gel interface, and the electrode−skin interface were electrically characterized by impedance spectroscopy; the electrode system's open circuit potential (OCP) was determined; steady-state visually evoked potentials (SSVEPs) and alpha waves were also captured by the electrode to determine signal quality as proposed by Li et al. [46].

2. Materials and methods

2.1. Manufacture of the electrode system

The complete electrode system consists of a 3D-printed, silver-coated PLA electrode body, which is embedded into a PVA−glycerol−NaCl contact gel that serves as an ionic bridge toward the human skin.

2.1.1. Gel production method

For the production of the gels, 4.5 g of polyvinyl alcohol (Acros, 98.0−98.8% hydrolyzed, 50−85 kDa) was added to 25.5 g, 1:1 ratio mixture of distilled water and glycerol (99.5%, Molar Chemicals Ltd.). It was stirred and heated to near boiling temperature in a beaker for 2 h; it was covered with a watch glass so only minimal amounts of water could evaporate. After the 2 h, 0.3 g plant-based activated charcoal powder was added during heavy stirring; 10 min later, 3 g of NaCl (analytical grade, Spektrum-3D Ltd.) was slowly mixed with the polymer solution, and then after a half minute of stirring, the solution was poured into molds, before it could solidify. The filled molds were then placed into sealable low−density polyethylene jars for a day; this allowed liquid to leak between the

Fig. 3. Production steps of the electrode system: printed PLA electrode body (top left); silver paint-coated PLA electrode body (bottom left); AgPLA placed into the 3D printed mold (middle); AgPLA fixed inside the cast PVA gel (right).
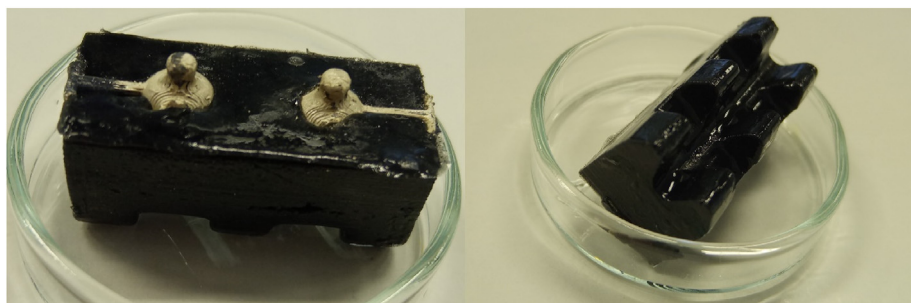
Fig. 4. Complete electrode system from the top (left) and the bottom (right).
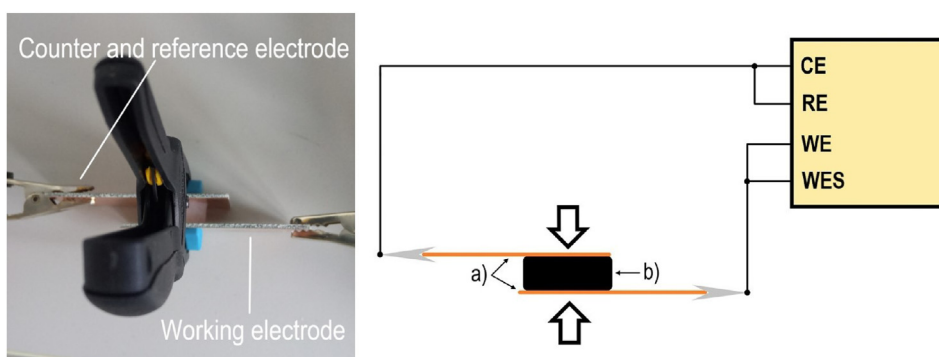

Fig. 5. Photo (left) and schematic figure (right) depicting the setup of the electrochemical impedance spectroscopic measurement determining the resistance of the PVA gel. CE — counter electrode; RE — reference electrode; WE — working electrode; WES — working electrode sense; (a) polished copper plates; (b) PVA gel; the big arrows indicate the plastic clamp.
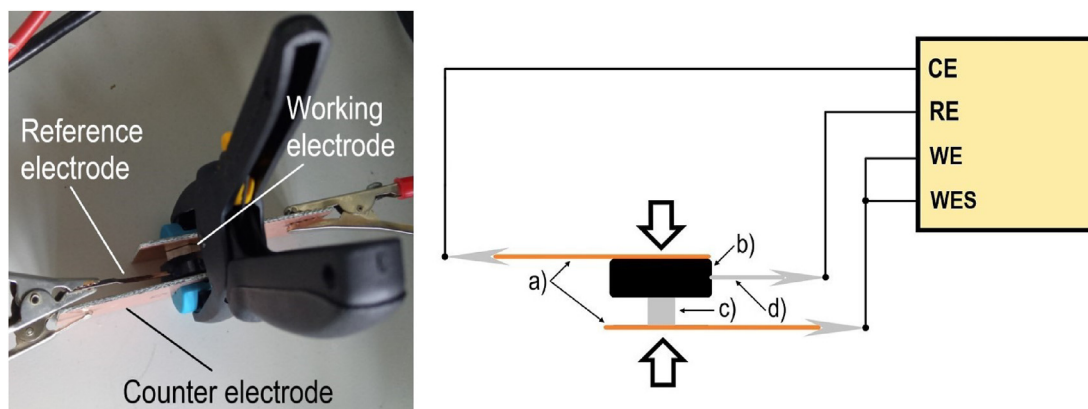

Fig. 6. Photo (left) and schematic figure (right) depicting the setup of the electrochemical impedance spectroscopic measurement carried out on a PVA gel-AgPLA interface. CE — counter electrode; RE — reference electrode; WE —working electrode; WES — working electrode sense; (a) polished copper plates; (b) PVA gel; (c) silver-coated PLA cube; (d) silver quasi-reference electrode; the big arrows indicate the plastic clamp.

solid gel and the wall of the mold, which made the removal of the whole hydrogel feasible. For impedance spectroscopic measurements regarding the characterization of the sole gel and the PVA gel−AgPLA interface, 12 welled polystyrene culture plates were used as molds providing cylindrical gels. The molds used for manufacturing complete electrodes were designed in Fusion 360 and were 3D printed by a Formlabs Form 2 printer using their standard black resin (Fig. 1). For this report, only one electrode geometry was considered.

2.1.2. Printing and coating of the electrode body

The PLA bodies were designed in Fusion 360 and were printed by an Original Prusa i3 MK3 printer, using PLA Extrafill Vertigo Gray and PLA Extrafill Metallic Grey filaments (Fillamentum Manufacturing Czech s.r.o.) (Fig. 2). They were designed to be used with snap connections and to have two positioning arms; the former enables fast setup and easy electrode swapping, the latter aids their fixation during the gel casting process. The bodies were printed in a 45° angle giving snaps resistance against breaking. PLA cubes of 1 cm^3 were also produced for the electrical investigation of the PVA gel−AgPLA interface. The coating process was carried out with a small paintbrush and silver paint (Demetron GmbH): the bodies were painted once with one loaded brush and once more with another — after a few minutes of drying — for better coverage. After the paint completely dried, the PVA-based gel was casted around the AgPLA body. We
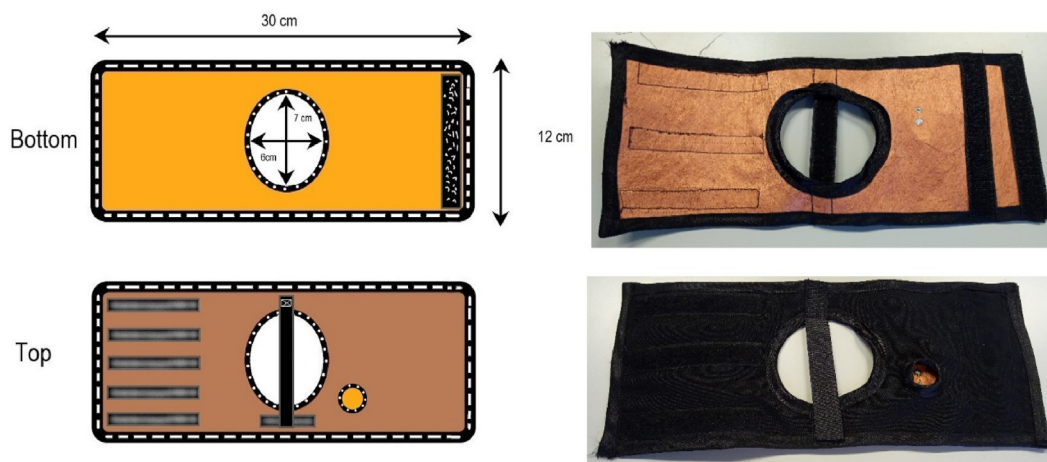
Fig. 7. Schematics of the wristband used for electrode−skin impedance spectroscopic measurements (left) and pictures of the manufactured design (right).
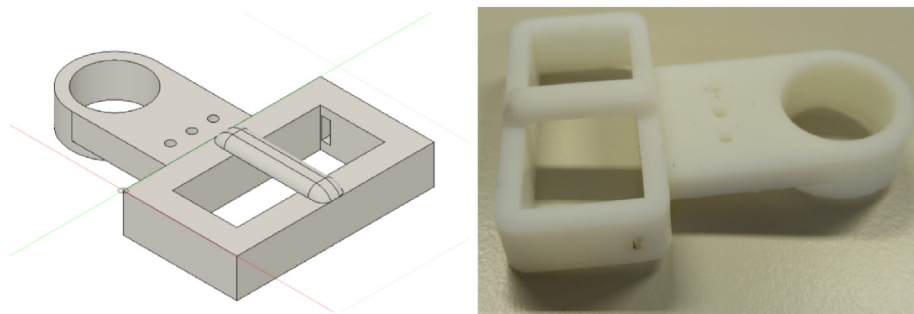

Fig. 8. Designed frame for holding the working and the quasi-reference electrodes, schematics on the left, the 3D-printed object on the right.
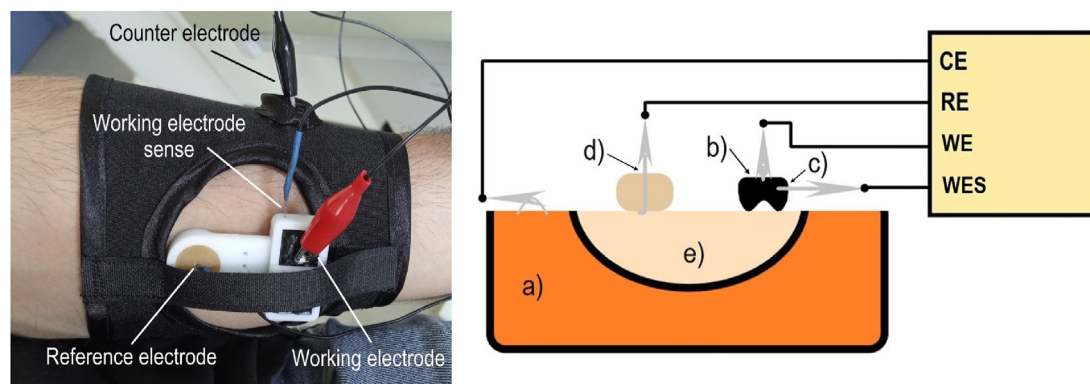

Fig. 9. Photo of the wristband and the electrode holding frame (left) and schematic figure (right) depicting the setup during the impedance measurements of the electrode-skin interface (without the insulating top layer). CE − counter electrode; RE − reference electrode; WE −working electrode; WES − working electrode sense; (a) copper-plated fabric; b) PVA gel-AgPLA electrode system; c) silver quasi-reference electrode; d) silver quasi-reference electrode transfixed through a silicone cylinder; e) skin of the subject; the big arrows indicate the plastic clamp.

investigated whether different surface treatments on the AgPLA body have any effect on the electrical properties of the PVA gel−AgPLA interface. The three treatments were the following: (1) the AgPLA was stored in 1 M NaCl solution for a week; (2) the electrode body was placed beside 1 M hydrochloric acid in a closed container also for a week; (3) nanoporous silver was electrochemically deposited on the surface of the coated body from $AgNO_3/HNO_3$ solution.

2.1.3. Assembly of the electrode system

The production steps of the electrode system can be followed in Fig. 3. The PLA body is first printed, and the printing supports are removed; this was followed by the coating with silver paint. After the paint has dried, the positioning arms of the AgPLA is placed into the indentations on the shorter sides of printed mold's cavity. The PVA solution is prepared as described in Chapter 2.1.1 and poured into the mold until the electrode body is almost wholly covered,

and only the snap connectors are left exposed. The finished electrode system can be seen in Fig. 4.

2.2. Electrochemical impedance spectroscopic (EIS) measurements

The electrical properties of the electrode system were characterized comprehensively via electrochemical impedance spectroscopy by a Zahner IM6e potentiostat. Since hydrogels are sensitive to the air's water content and thus are prone to dehydration when left on open air, the PVA gels' resistance change was investigated during aging in open containers and also when stored in environments with set humidity. In the case of the former, gels were stored at 25 °C room temperature in a laminar flow box with the humidity level uncontrolled. The impedance spectroscopic measurements were carried out on fresh gels after 5 and 25 days of exposure to the open air. Two sets of PVA gels (n = 4) were placed into two desiccators. One of them contained a jar filled with distilled water to maintain 100% humidity, while the other one filled with saturated MgCl$_2$ (hexahydrate, AR; Reanal Inc.), providing 33% humidity level. Each set of gels was kept in one of the desiccators for a whole week, while their mass and conductivity were measured each day. After a week, the PVA gels were swapped, and the experiment continued for one more week. During the EIS measurements, the cylindrical solid gels with 2 cm diameter were placed between two polished copper plates and fixed with a plastic clamp, after excess fluid has been wiped off. In these experiments, the potentiostat was used in a two-electrode configuration, that is, the counter and the reference electrode leads tied together was connected to one plate while the working and working sense connections to the other one (Fig. 5). The perturbing amplitude was chosen to be 10 mV in this and every other EIS measurements, the investigated frequency range was 10 Hz−100 kHz starting from the high values. If the high frequency values of the impedance spectra are constant, then these represent the resistance of the system.
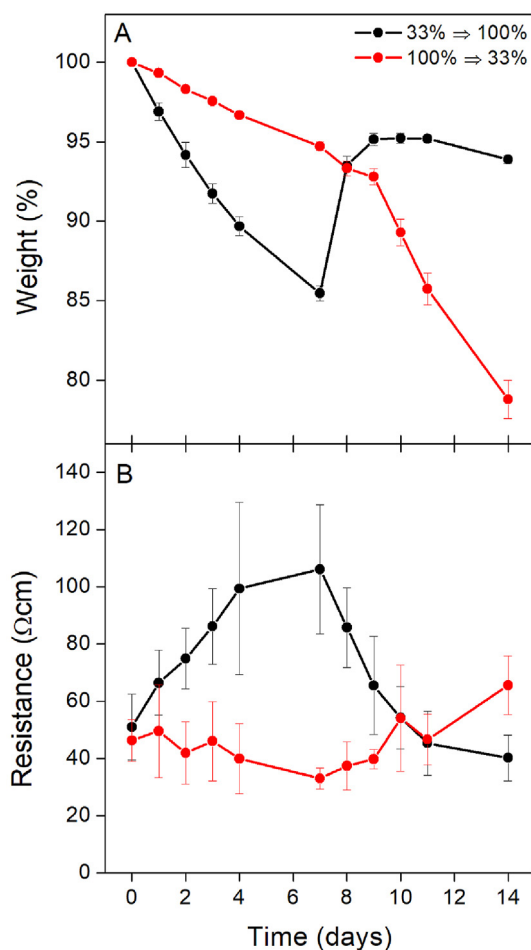
The interface of PVA gels and the AgPLA bodies was also examined. For this measurement, coated PLA cubes were immersed 4.5 mm deep into cylindrical PVA gels before complete solidification. These coupled systems were also placed between the same two polished copper plates fixed with a plastic clamp as before, one of them serving as the contact to the silver-coated working electrode, while the other one being the counter electrode. In this case, the measurement was carried out in a three-electrode configuration, that is, a silver wire as quasi-reference electrode was inserted into the hydrogel phase (Fig. 6). The investigated frequency range was between 10 mHz and 100 kHz.

Finally, the impedance values of the electrode−skin interface were determined, which is the most decisive factor of electrode
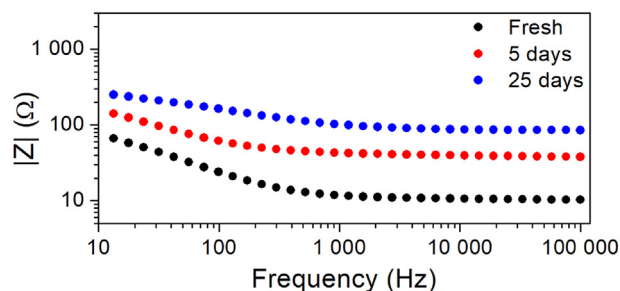
qualification, besides signal quality. This experiment was carried out with the help of eleven volunteers using the final electrode design (n = 3) and a custom-made wristband. The wristband was made from a 12 cm × 30 cm layer of copper-plated fabric (LORIX Ltd., Budapest, Hungary) sewn together with a similarly sized layer of plastic textile and a few strips of touch fastener. The band had a 6 cm × 7 cm oval opening in the middle of it, and the upper non-conductive layer had a smaller circular hole to give access to the copper-plated fabric (Fig. 7). After fastening the band on the volunteer's forearm, a 3D-printed frame was placed into the opening that held the PVA gel-AgPLA electrode and a piece silver wire transfixed through a silicone cylinder, which was used as the quasi-reference electrode (Fig. 8). The frame holding the electrodes was fixed with another strip of touch fastener reaching across the opening. In this case, a four-electrode configuration was used: the working electrode sense lead was connected to a silver wire quasi-reference electrode inserted into the side of the hydrogel, while the other silver wire quasi-reference electrode was pushed against the skin of the volunteer and connected to the reference electrode lead. The working electrode lead was connected to the silver-coated snap connector of the examined electrode system; the counter electrode led to the copper fabric through the small hole on the upper layer. The complete setup can be seen in Fig. 9. The investigated frequency range during this measurement was 1 Hz−100 kHz. The

Fig. 10. Results of the impedance measurements of bulk gels: effect of aging on the resistance. The impedance values stay constant above a few kHz; thus, those values can be considered as the resistance of the gel samples. The corresponding specific resistivity values are 46 Ωcm, 171 Ωcm, and 384 Ωcm, respectively.

Fig. 11. The weight (A) and resistance (B) change of PVA gels kept in a desiccator with 33% humidity for a week, then in one with 100% for another week (black). Gels kept in the same desiccators in the reverse order (red) are also depicted.

electrode—skin impedance measurements were conducted just before the alpha wave detection, except the 3-hour-long experiment, which was done separately.

In order to eliminate the effect of electrode surface area on the resistance and impedance, area-normalized values were calculated. Since the proposed electrode has a highly porous hydrogel as the contact material, only geometric area-normalized parameters were feasible to be assessed. Specific resistance of the PVA gels was calculated individually using the volume of the cylinders. The diameter of their bases was changing slightly during dehydration, so an average of 2 cm was chosen giving an area of 3.141 cm^2. The height of the cylinder was slightly different between specimen. During the silver treatment studies, the PVA gel—AgPLA interface was roughly 2.8 cm^2. Estimating the electrode area in the case of electrode—skin impedance measurements was the most difficult, since here two soft materials established an interface deforming each other. This parameter was approximated by the area of the mark on the skin left by the electrode, which was 1.1 cm^2. This presentation of electrode impedances enables comparison with other semi-dry EEG electrode designs [47].

2.3. Open circuit potential and potential drift

To characterize the *dc* properties of the proposed electrodes the OCP was recorded using a Zahner IM6ex potentiostat in conjunction with a Zahner Noise Probe. The OCP values of the sintered Ag/AgCl electrodes used in the EEG measurements were also investigated. The electrodes (n = 3) were immersed in 3% saline solution, and the OCP was recorded for 10 min at 20.48 Hz sampling rate against a reference Ag/AgCl (CHI111, CH Instruments Inc.) electrode.

2.4. EEG recordings

To determine the achievable signal quality of the proposed electrode design, electroencephalographic measurements were carried out with two approaches that are most commonly used for EEG-based BCI system characterization: recording of SSVEPs and alpha wave detection. For these experiments, a MindRove Arc headset (MindRove Kft., Budapest, Hungary) has been modified by the engineers of the company. The printed circuit board contains a 24-bit resolution A/D converter, which was configured to record voltage signals with a 500 Hz sampling rate.

2.4.1. SSVEP recordings

SSVEPs are such evoked potentials that can be detected from the visual cortex in response to a visual stimulus; the frequency of the signal matches that of the stimulus. With this approach, the achievable signal-to-noise ratio (SNR) is rather high and is also applicable in the case of same-place-different-time detection method [48]. During this experiment, three different PVA gel-AgPLA electrodes were inserted into the headband's snap connections for each of the three selected volunteer, then it was placed on their head in a way that the electrodes touched the scalp at the occipital area, one in the middle and one on either side of it. After fixing the band on the head, the electrodes were moved up-and-down and side-to-side slightly to brush the hair aside and to make the connection with the scalp as good as possible. For reference electrode and driven right leg (DRL) lead conventional Ag/AgCl EEG electrodes were used with conductive gel (Parker Laboratories Inc. SignaGel®) and were placed under both ears on the neck. The visual stimulus was given by a row of three LEDs connected to an Arduino microcontroller with the frequency set to 20 Hz. The volunteers were asked to look at the blinking LEDs for 1 min. The measurements were repeated every 30 min during a 3-hourlong session. During this time, the headband was not removed;

only the reference electrodes were adjusted and filled with conductive gel when needed.

2.4.2. Alpha wave detection

Alpha rhythm is a neural oscillation in the frequency band of 8—12 Hz that is dominant during wakeful relaxation, while the eyes are closed. Because of its large amplitude, it can be detected throughout the scalp, which makes the alpha wave detection applicable in same-time-different-place recording approach. Thus, this method was used to compare the proposed electrode design with the conventional Ag/AgCl electrodes in regard of short- and long-term signal quality. For the measurement, the headband was setup similarly to the SSVEP recordings; the difference was that only one PVA gel-AgPLA electrode was used and placed on the right side of the occipital area and beside it on the left side an Ag/AgCl electrode filled with conductive gel was positioned. The alpha wave detection was conducted for 3 h with three and 1 h with eight more volunteers. Every 30 min, the volunteers were asked to sit still for 2 min eyes closed and after that with their eyes open for 2 min as well. The volunteers in this experiment were the same as the ones partaking in the electrode—skin impedance measurement.

3. Results and discussion

3.1. PVA gel-AgPLA electrode system development

Previously, PVA gels using the freezing-thawing method were produced, but the hydrogels obtained this way were greatly susceptible to dehydration and mold formation. The latter could be prevented with the use of fungistatics. However, the solution of the problem regarding dehydration required a different manufacturing approach [29,45]; hence, we started using the mixture of glycerol and distilled water as the solvent of PVA. The production method described earlier resulted in hydrogels that have high conductivity (see Section 3.2), possess excellent mechanical properties, and are less susceptible to dehydration than their water-based counterparts. Using only water or low glycerol/water ratio leads to a high degree of dehydration and shrinkage, while the proposed 1:1 ratio alleviates this greatly. Fresh hydrogels had an average diameter of 20.5 mm; this reduced to an average of 19.2 mm after being left on open air (uncontrolled humidity, 25 °C) for a month and kept this size indefinitely. After drying out in the described way, the PVA gels did not dehydrate completely; they maintained most of their flexibility although they became more prone to tearing when put under high stress. In order to maintain optimal mechanical and electrical properties the gels should be stored in airtight containers with high humidity (see Section 3.2.2), this way a shelf life of several months can be achieved. It should also be noted that while the PVA gel-AgPLA electrode is a reusable system, an individual
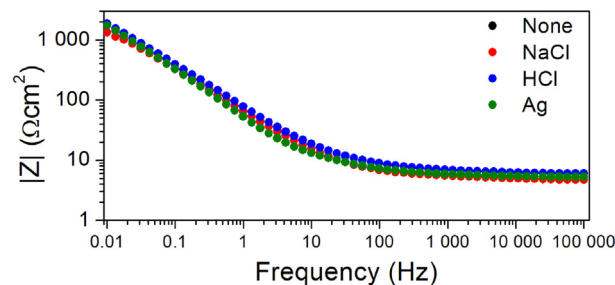

Fig. 12. Results of EIS measurements on PVA gel-AgPLA interfaces. The different treatments did not yield significant improvement on the specific impedance values.
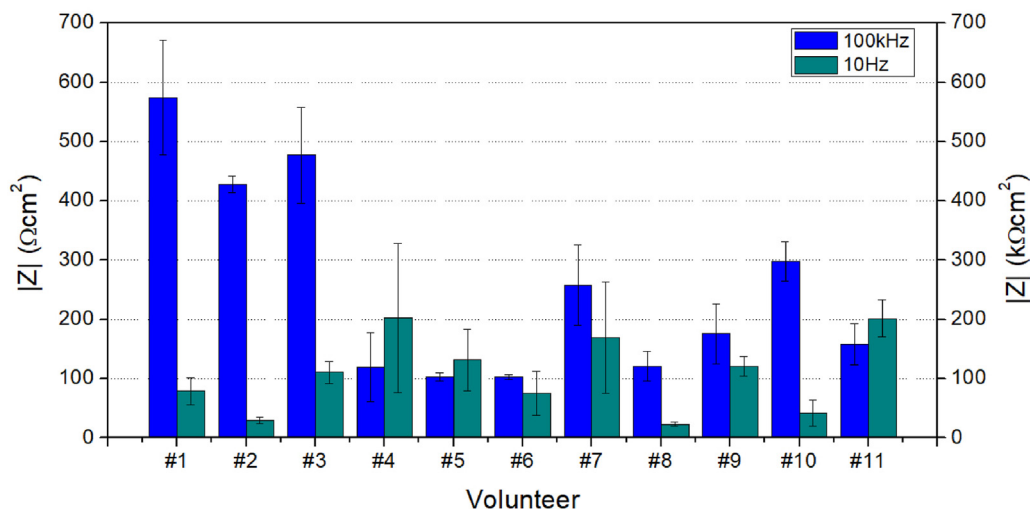
Fig. 13. Average electrode−skin interface impedance values at 100 kHz (in Ωcm^2, blue) and at 10 Hz (in $k\Omega cm^2$, dark cyan) for all 11 volunteers.

electrode should only be used by one person due to proper hygiene and health considerations.

In preliminary experiments, potassium chloride was investigated as a substitute for sodium chloride, but since it had a stronger "salting-out" effect, the potassium salt caused immediate gelation, which prevented the casting of the solution. The added charcoal was mainly used to dye the gels black, but it also eliminated most of the air bubbles generated during stirring. Since it was added in a very small amount, it had no effect on the gels' electrical properties.

3.2. Characterization of the PVA gel-AgPLA electrode system

3.2.1. Effect of PVA gel aging on resistance

Fig. 10 shows the result of the EIS measurements conducted on the PVA gels stored in an open container on the example of one selected gel at all three timestamps. Even though the resistance, which corresponds to the constant high frequency impedance values, increased tenfold after 25 days, it still remained below 400 Ωcm. These results show the PVA gel's moderate sensitivity to aging, but for achieving longer shelf life, the electrodes should be kept in a sealed container when not used.

3.2.2. Effect of controlled humidity on PVA gel resistance and swelling

Because of the hydrogels' sensitivity to their environment, especially humidity, it is important to assess its extent. The PVA gels kept in 33% humidity gradually lost their water content, which led to shrinkage and increase in resistance. After these were placed into 100% humidity environment, the gels swollen back up and the resistance values decreased. Excess fluid was also observable around and on them. In this highly humid milieu, the PVA gels
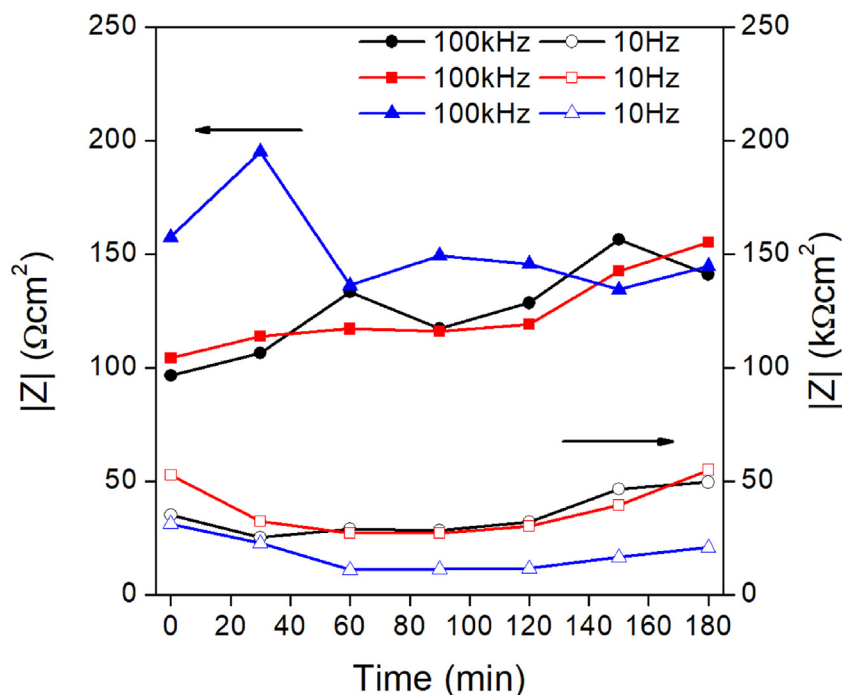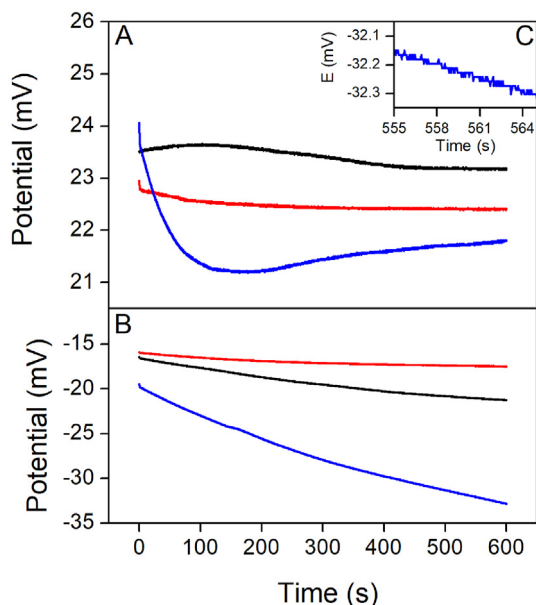

Fig. 14. Electrode−skin interface impedance values at 100 kHz (in Ωcm^2) and at 10 Hz (in $k\Omega cm^2$) recorded during the long-term measurement.
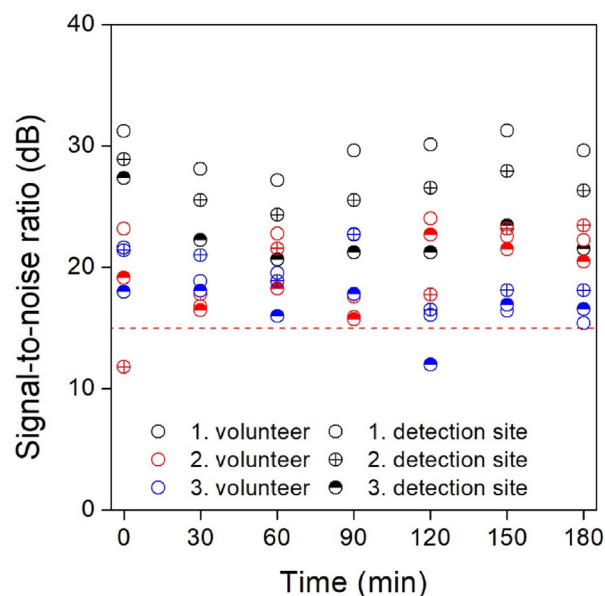
Fig. 15. Open circuit potential of the sintered Ag/AgCl electrodes (A) and the PVA gel-AgPLA electrodes (B) during 10-minute measurement in the 3% saline solution. Noise levels of a PVA gel-AgPLA electrode during 10 s (C).


Fig. 17. Signal-to-noise ratios of the SSVEP signals for every patient and detection site. The acceptability limit of 15 dB is marked with a dotted red line.

slowly decreased in weight which can be attributed to the removal of excess salty fluid prior to the EIS measurements. These changes in weight and resistance can be seen in Fig. 11.

3.2.3. Effect of AgPLA surface treatments on impedance of the PVA gel-AgPLA interface

The silver coating on the PLA electrode body lost its metallic shine after the gel was cast around it and was left in the sealable container. This phenomenon is due to silver chloride formation on the surface of the coating. Three treatment methods were applied to the AgPLA bodies to investigate the potential enhancement of electrical properties; these are described in detail in Chapter 2.1.2. These treatments, however, did not yield positive results; the obtained impedance spectra were almost identical to that of the untreated AgPLA bodies (Fig. 12). Even though a more sophisticated AgCl production method was not employed, such as the procedures proposed by Polk et al. [49] and Lito et al. [50] the PVA gel-AgPLA interface possessed significantly lower impedance compared to

that of the gel−skin interface. As a consequence, surface treatment of the silver was omitted in the final process.

3.2.4. Electrode−skin interface impedance

The results of the electrode−skin impedance spectroscopy showing the average impedance values at 100 kHz and 10 Hz for each volunteer can be seen in Fig. 13. There are significant differences observable between these measured values at 10 Hz; the volunteer with the lowest electrode−skin impedance had around 20 kΩcm^2, while the highest reached 200 kΩcm^2. This can mainly be attributed to different skin types and other underlying factors such as hydration. In order to lower the impedance, some conductive liquid on the surface of the gel and the reference electrode or slight abrasion to the _stratum corneum_ could be applied. Fig. 14 shows the data related to the long-term electrode−skin measurements. These results show that the impedance at high
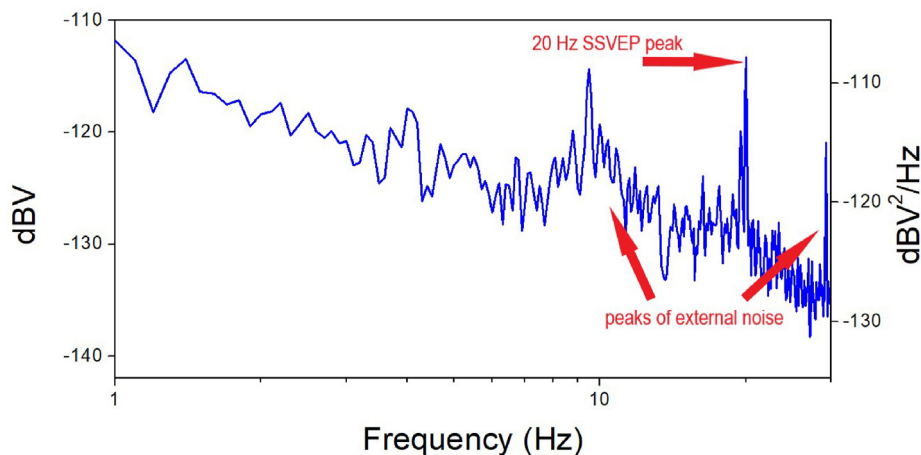
Fig. 16. Fourier spectra of steady-state visually evoked potential detection recorded with PVA gel-AgPLA electrodes. The 20 Hz peak and the external noise are marked with red arrows.
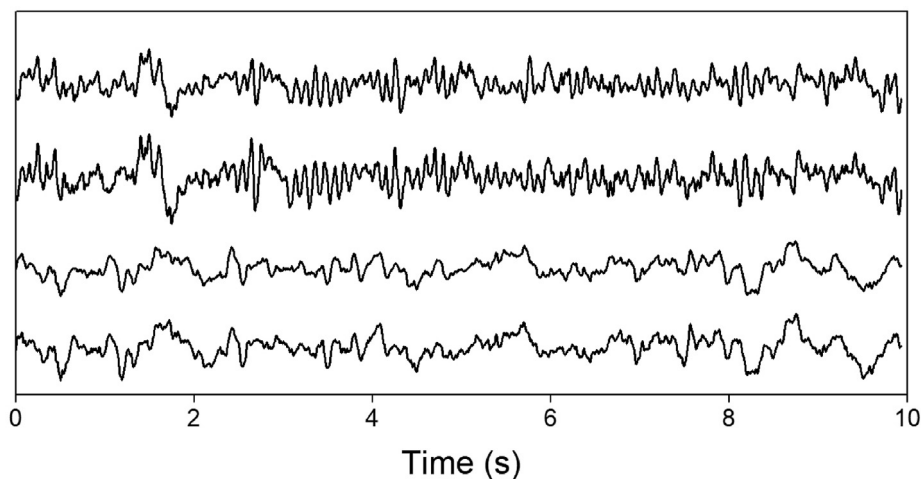
Fig. 18. Temporal spectra of alpha wave detection recorded with conventional Ag/AgCl electrode (1 and 3) and PVA gel-AgPLA electrode (2 and 4) with eyes open (1 and 2) and closed (3 and 4). The signals were filtered with averaging filter (n = 34).

frequency increases with time, but at 10 Hz, it decreases first before the increase. This is due to the initial wetting of the skin, followed by the slow dehydration of the gel. However, the signal quality is a more important factor for determining the electrode design's usability as an EEG sensor than the electrode−skin impedance.

3.2.5. Open circuit potential and potential drift

OCP was calculated by averaging the 10-min-long recordings; potential drift was obtained by the difference between the maximum and minimum values. The sintered Ag/AgCl electrodes had a mean OPC of 22.49 mV with a standard deviation of 0.9 mV, and the PVA gel-AgPLA electrodes showed an average of −21.22 mV and a standard deviation of 5.43 mV. The potential drift was 1.32 ± 1.36 mV for the former and 6.60 ± 6.09 mV for the latter. The negative potential of the PVA gel-AgPLA electrode increased with time (as seen in Fig. 15), which is due to the ongoing ion diffusion between the gel and the saline solution. The data obtained with the proposed electrodes are somewhat less favorable as compared to those with the sintered Ag/AgCl ones. However, we would like to emphasize that the aimed application field is the BCI where signals in the frequency range above 0.5 Hz are significant and those values of the OCP and drift are acceptable.

3.3. EEG recordings

The recorded EEG signals were processed via MATLAB scripts. The first step was to extract uniform length of recording; in the case of SSVEP signal acquisition, this was chosen to be 30 s of data exempt from motion artefacts. For alpha wave detection, 1-min-long records were picked. Next, the data were subjected to Fourier transformation to gain the frequency spectra.

The SNR of the evoked potentials was gained in the following way: the amplitude value of the 20 Hz peak (signal) was divided by the standard deviation of the values in the 21−29 Hz frequency range (noise); then it was converted into decibel:

$$SNR_{dB} = 20 \log(\sigma_{signal} / \sigma_{noise}) \tag{1}$$

The frequency spectrum of one measurement can be seen in Fig. 16. In Fig. 17., all the SNR values are shown. The deviations are mainly due to different detection sites, hair lengths, and skin types. The gained SNRs are almost exclusively above 15 dB, which can be considered a limit to acceptable SNR values.

The temporal spectra of the measurements regarding the alpha wave activity are depicted in Fig. 18. The heightened alpha wave
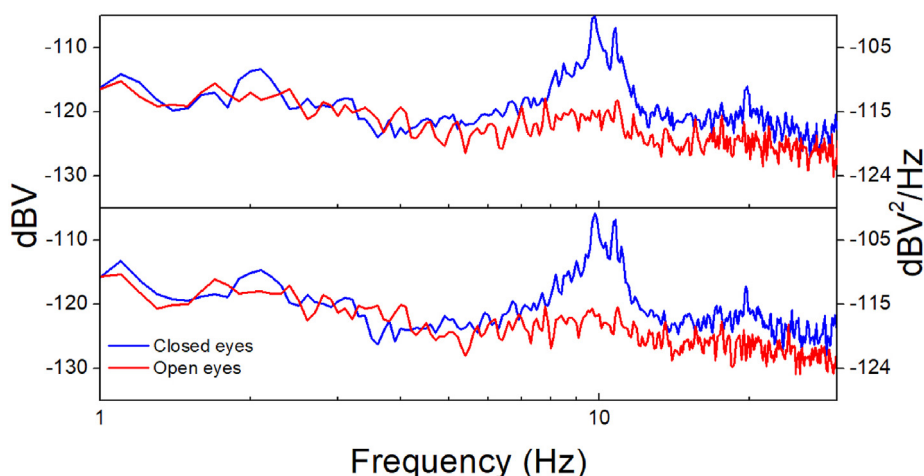
Fig. 19. Fourier spectra of alpha wave detection recorded with conventional Ag/AgCl (top) and PVA gel-AgPLA (bottom) electrode with eyes closed and open.
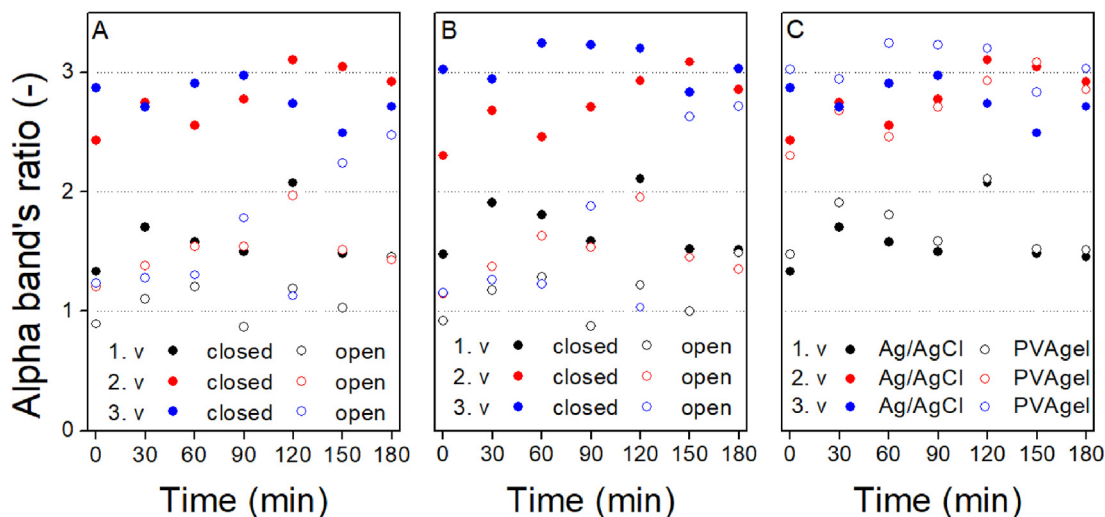
Fig. 20. Alpha band's ratio values of the conventional wet Ag/AgCl electrodes (A), the PVA gel-AgPLA electrodes (B) in the case of long-term alpha wave recordings. Comparison of the conventional Ag/AgCl and the PVA gel-AgPLA electrodes in regard to alpha band's ratio values recorded during closed eyes (C). (v − volunteer).
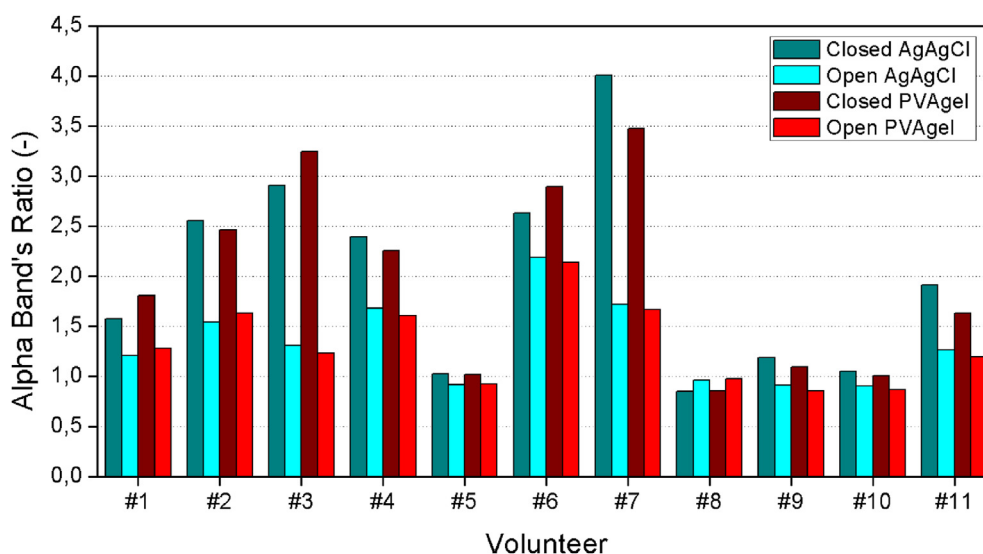

Fig. 21. Alpha band's ratio values of both electrodes, with eyes open and closed at the 1-hour mark of the alpha wave recordings for all volunteers.

activity during closed eyes can be observed in Fig. 19. in the case of the wet Ag/AgCl and the PVA gel-AgPLA electrodes, respectively. We chose the determination of alpha band's ratios (ABR) as a way to

Table 1
Correlation coefficients between the data recoded by Ag/AgCl and PVA gel-AgPLA electrodes using same-time-different-place method for alpha wave capture.

Volunteer	Closed eyes			Open eyes		
	0 h	0.5 h	1 h	0 h	0.5 h	1 h
1	0.84	0.84	0.78	0.77	0.74	0.78
2	0.95	0.95	0.87	0.81	0.87	0.87
3	0.81	0.88	0.85	0.78	0.83	0.71
4	0.79	0.89	0.94	0.94	0.94	0.93
5	0.78	0.95	1.00	0.95	0.92	0.93
6	0.69	0.82	0.83	0.81	0.84	0.84
7	0.90	0.93	0.86	0.79	0.88	0.82
8	0.33	0.89	0.96	0.89	0.88	0.98
9	0.79	0.84	0.86	0.88	0.87	0.83
10	0.94	0.86	0.82	0.74	0.82	0.84
11	0.62	0.86	0.09	0.80	0.83	0.92

quantify this enhanced activity. ABR was calculated by dividing the mean of the amplitudes in the alpha range (8−12 Hz) by the means of two adjacent frequency regions (5−7 Hz and 13−15 Hz). The ABR values regarding the 3-hour-long measurements for the conventional Ag/AgCl and the PVA gel-AgPLA electrodes calculated this way are shown in Fig. 20A and B, respectively. The two sensors can be compared in this regard with the help of Fig. 20C. The ABR values after 1 h of wearing the headset are shown in Fig. 21 for all 11 volunteers and both electrodes. The difference in signal quality between volunteers can mainly be attributed to different skin types, hair length, and neural activity; the PVA gel-AgPLA electrodes work better on sites with shorter hair, just like the conventional wet electrodes do. The electrode−skin impedance values also showed no correlation with the ABR. As time went on, the difference between ABR values obtained by closed and open eyes show a narrowing tendency, which can be attributed to the long nature of the experiment. The volunteers presumably lost interest in the lengthy measurement, due to this strong alpha waves were detectable even with eyes open. The electrode−skin impedance

values also showed no correlation with the ABR. Comparing our electrode system to the conventional wet electrode, we can conclude that the signal quality is very similar, the proposed design is on par with the golden standard. The Pearson correlation coefficient was also determined between the datasets recorded at the same time with different electrodes, which is show in Table 1. The grand average of the coefficients is 0.83. There are two values here that are significantly lower than the rest, which is most likely due to motion artefacts.

4. Conclusion

Reusable electrode system for non-invasive BCI application has been developed. Polyvinyl alcohol−glycerol−NaCl contact hydrogel and 3D-printed, silver-coated PLA electrode body has been produced and assembled. The use of gel casting and 3D printing techniques makes the manufacture of the electrode system easy, fast, and cheap. Additionally, they provide great freedom in sensor geometry enabling good and comfortable skin contact on hairy sites of the scalp, the application is also simple due to the snap connectors. Because of the high glycerol content, the PVA gels are resistant to dehydration and mold formation, ensuring reusability and long shelf life. The signal quality is adequate and is comparable with that of the conventional wet electrodes even at long term. Results from electroencephalographic measurements, such as SSVEP and alpha wave detection, verify the electrode system for BCI use.

CRediT author statement

Kristóf Jakab: Conceptualization, Methodology, Software, Formal analysis, Investigation, Writing − Original Draft, Writing − Review and Editing. **János Csipor**: Investigation, Software. **István Ulbert**: Funding acquisition, Writing − Review and Editing. **Zsófia Keresztes**: Resources, Writing − Review and Editing. **Gábor Mészáros**: Conceptualization, Validation, Methodology, Writing − Review and Editing. **Gergely Márton**: Conceptualization, Resources, Writing − Review and Editing.

Data availability

The raw data required to reproduce these findings are available to download from https://data.mendeley.com/datasets/66ndcswhr2/3. The processed data required to reproduce these findings are available to download from https://data.mendeley.com/datasets/2rr75x4wg4/2.

Declaration of competing interest

The authors declare that they have no known competing financial interests or personal relationships that could have appeared to influence the work reported in this paper.

Acknowledgment

References

[1] D.J. McFarland, J.R. Wolpaw, EEG-based brain−computer interfaces, Curr. Opin. Biomed. Eng. 4 (2017) 194−200, https://doi.org/10.1016/j.cobme.2017.11.004.

[2] S.N. Abdulkader, A. Atia, M.S.M. Mostafa, Brain computer interfacing: applications and challenges, Egypt, Informatics J 16 (2015) 213−230, https://doi.org/10.1016/j.eij.2015.06.002.

[3] R. Wang, X. Jiang, W. Wang, Z. Li, A microneedle electrode array on flexible substrate for long-term EEG monitoring, Sensor. Actuator. B Chem. 244 (2017) 750−758, https://doi.org/10.1016/j.snb.2017.01.052.

[4] P. Griss, H.K. Tolvanen-Laakso, P. Meriläinen, G. Stemme, Characterization of micromachined spiked biopotential electrodes, IEEE Trans. Biomed. Eng. 49 (2002) 597−604, https://doi.org/10.1109/TBME.2002.1001974.

[5] N.S. Dias, J.P. Carmo, A.F. Da Silva, P.M. Mendes, J.H. Correia, New dry electrodes based on iridium oxide (IrO) for non-invasive biopotential recordings and stimulation, Sensors Actuators, A Phys. 164 (2010) 28−34, https://doi.org/10.1016/j.sna.2010.09.016.

[6] G. Ruffini, S. Dunne, L. Fuentemilla, C. Grau, E. Farrés, J. Marco-Pallarés, P.C.P. Watts, S.R.P. Silva, First human trials of a dry electrophysiology sensor using a carbon nanotube array interface, Sensors Actuators, A Phys. 144 (2008) 275−279, https://doi.org/10.1016/j.sna.2008.03.007.

[7] S. Krachunov, A.J. Casson, 3D printed dry EEG electrodes, Sensors (Basel) 16 (2016), https://doi.org/10.3390/s16101635.

[8] P. Salvo, R. Raedt, E. Carrette, D. Schaubroeck, J. Vanfleteren, L. Cardon, A 3D printed dry electrode for ECG/EEG recording, Sensors Actuators, A Phys. 174 (2012) 96−102, https://doi.org/10.1016/j.sna.2011.12.017.

[9] X. Guo, W. Pei, Y. Wang, Q. Gui, H. Zhang, X. Xing, Y. Huang, H. Chen, R. Liu, Y. Liu, Developing a one-channel BCI system using a dry claw-like electrode, in: Proc. Annu. Int. Conf. IEEE Eng. Med. Biol. Soc. EMBS. 2016-Octob, 2016, pp. 5693−5696, https://doi.org/10.1109/EMBC.2016.7592019.

[10] A. Velcescu, A. Lindley, C. Cursio, S. Krachunov, C. Beach, C.A. Brown, A.K.P. Jones, A.J. Casson, Flexible 3D-printed EEG electrodes, Sensors (Switzerland) 19 (2019) 1−14, https://doi.org/10.3390/s19071650.

[11] K.P. Gao, H.J. Yang, X.L. Wang, B. Yang, J.Q. Liu, Soft pin-shaped dry electrode with bristles for EEG signal measurements, Sensors Actuators, A Phys. 283 (2018) 348−361, https://doi.org/10.1016/j.sna.2018.09.045.

[12] Y.H. Chen, M. Op de Beeck, L. Vanderheyden, E. Carrette, V. Mihajlović, K. Vanstreels, B. Grundlehner, S. Gadeyne, P. Boon, C. van Hoof, Soft, comfortable polymer dry electrodes for high quality ECG and EEG recording, Sensors (Switzerland) 14 (2014) 23758−23780, https://doi.org/10.3390/s141223758.

[13] Y. Wu, P. Deng, Y. Tian, J. Feng, J. Xiao, J. Li, J. Liu, G. Li, Q. He, Simultaneous and sensitive determination of ascorbic acid, dopamine and uric acid via an electrochemical sensor based on PVP-graphene composite, J. Nanobiotechnol. 18 (2020) 1−13, https://doi.org/10.1186/s12951-020-00672-9.

[14] Y. Wu, P. Deng, Y. Tian, Z. Ding, G. Li, J. Liu, Z. Zuberi, Q. He, Rapid recognition and determination of tryptophan by carbon nanotubes and molecularly imprinted polymer-modified glassy carbon electrode, Bioelectrochemistry 131 (2020) 107393, https://doi.org/10.1016/j.bioelechem.2019.107393.

[15] Y. Wu, G. Li, Y. Tian, J. Feng, J. Xiao, J. Liu, X. Liu, Q. He, Electropolymerization of molecularly imprinted polypyrrole film on multiwalled carbon nanotube surface for highly selective and stable determination of carcinogenic amaranth, J. Electroanal. Chem. 895 (2021), 115494, https://doi.org/10.1016/j.jelechem.2021.115494.

[16] C. Grozea, C.D. Voinescu, S. Fazli, Bristle-sensors - low-cost flexible passive dry EEG electrodes for neurofeedback and BCI applications, J. Neural. Eng. 8 (2011), https://doi.org/10.1088/1741-2560/8/2/025008.

[17] C.T. Lin, L. De Liao, Y.H. Liu, I.J. Wang, B.S. Lin, J.Y. Chang, Novel dry polymer foam electrodes for long-term EEG measurement, IEEE Trans. Biomed. Eng. 58 (2011) 1200−1207, https://doi.org/10.1109/TBME.2010.2102353.

[18] L. De Liao, I.J. Wang, S.F. Chen, J.Y. Chang, C.T. Lin, Design, fabrication and experimental validation of a novel dry-contact sensor for measuring electroencephalography signals without skin preparation, Sensors 11 (2011) 5819−5834, https://doi.org/10.3390/s110605819.

[19] G. Li, J. Wu, Y. Xia, Y. Wu, Y. Tian, J. Liu, D. Chen, Q. He, Towards emerging EEG applications: a novel printable flexible Ag/AgCl dry electrode array for robust recording of EEG signals at forehead sites, J. Neural. Eng. 17 (2020), https://doi.org/10.1088/1741-2552/ab71ea.

[20] A.R. Mota, L. Duarte, D. Rodrigues, A.C. Martins, A.V. Machado, F. Vaz, P. Fiedler, J. Haueisen, J.M. Nóbrega, C. Fonseca, Development of a quasi-dry electrode for EEG recording, Sensors Actuators, A Phys. 199 (2013) 310−317, https://doi.org/10.1016/j.sna.2013.06.013.

[21] H.L. Peng, J.Q. Liu, H.C. Tian, Y.Z. Dong, B. Yang, X. Chen, C.S. Yang, A novel passive electrode based on porous Ti for EEG recording, Sensor. Actuator. B Chem. 226 (2016) 349−356, https://doi.org/10.1016/j.snb.2015.11.141.

[22] X. Xing, W. Pei, Y. Wang, X. Guo, H. Zhang, Y. Xie, Q. Gui, F. Wang, H. Chen, Assessing a novel micro-seepage electrode with flexible and elastic tips for wearable EEG acquisition, Sensors Actuators, A Phys. 270 (2018) 262−270, https://doi.org/10.1016/j.sna.2017.12.048.

[23] S. Toyama, K. Takano, K. Kansaku, A non-adhesive solid-gel electrode for a non-invasive brain-machine interface, Front. Neurol. JUL (2012) 1−8, https://doi.org/10.3389/fneur.2012.00114.

[24] P. Pedrosa, P. Fiedler, L. Schinaia, B. Vasconcelos, A.C. Martins, M.H. Amaral, S. Comani, J. Haueisen, C. Fonseca, Alginate-based hydrogels as an alternative to electrolytic gels for rapid EEG monitoring and easy cleaning procedures, Sensor. Actuator. B Chem. 247 (2017) 273−283, https://doi.org/10.1016/j.snb.2017.02.164.

[25] N.A. Alba, R.J. Sclabassi, M. Sun, X.T. Cui, Novel hydrogel-based preparation-free EEG electrode, IEEE Trans. Neural Syst. Rehabil. Eng. 18 (2010) 415−423, https://doi.org/10.1109/TNSRE.2010.2048579.

[26] G. Li, S. Wang, M. Li, Y.Y. Duan, Towards real-life EEG applications: novel superporous hydrogel-based semi-dry EEG electrodes enabling automatically "charge-discharge" electrolyte, J. Neural. Eng. 18 (2021), https://doi.org/10.1088/1741-2552/abeeab.

[27] P. Pedrosa, P. Fiedler, V. Pestana, B. Vasconcelos, H. Gaspar, M.H. Amaral, D. Freitas, J. Haueisen, J.M. Nóbrega, C. Fonseca, In-service characterization of a polymer wick-based quasi-dry electrode for rapid pasteless electroencephalography, Biomed. Tech. 63 (2018) 349−359, https://doi.org/10.1515/bmt-2016-0193.

[28] G. Li, D. Zhang, S. Wang, Y.Y. Duan, Novel passive ceramic based semi-dry electrodes for recording electroencephalography signals from the hairy scalp, Sensor. Actuator. B Chem. 237 (2016) 167−178, https://doi.org/10.1016/j.snb.2016.06.045.

[29] S. Peng, X. Jiang, X. Xiang, K. Chen, G. Chen, X. Jiang, L. Hou, High-performance and flexible solid-state supercapacitors based on high toughness and thermoplastic poly(vinyl alcohol)/NaCl/glycerol supramolecular gel polymer electrolyte, Electrochim. Acta 324 (2019), 134874, https://doi.org/10.1016/j.electacta.2019.134874.

[30] J. Ben, Z. Song, X. Liu, W. Lü, X. Li, Fabrication and electrochemical performance of PVA/CNT/PANI flexible films as electrodes for supercapacitors, Nanoscale Res. Lett. 15 (2020) 4−11, https://doi.org/10.1186/s11671-020-03379-w.

[31] H. Hosseini, S. Shahrokhian, Vanadium dioxide-anchored porous carbon nanofibers as a Na+ intercalation pseudocapacitance material for development of flexible and super light electrochemical energy storage systems, Appl. Mater. Today 10 (2018) 72−85, https://doi.org/10.1016/j.apmt.2017.11.011.

[32] C. Amri, M. Mudasir, D. Siswanta, R. Roto, In vitro hemocompatibility of PVA-alginate ester as a candidate for hemodialysis membrane, Int. J. Biol. Macromol. 82 (2016) 48−53, https://doi.org/10.1016/j.ijbiomac.2015.10.021.

[33] N. Imtiaz, M.B.K. Niazi, F. Fasim, B.A. Khan, S.A. Bano, G.M. Shah, M. Badshah, F. Menaa, B. Uzair, Fabrication of an original transparent PVA/gelatin hydrogel: in vitro antimicrobial activity against skin pathogens, Int. J. Polym. Sci. 2019 (2019) 1−11, https://doi.org/10.1155/2019/7651810.

[34] K. Pal, A.K. Banthia, D.K. Majumdar, Preparation and characterization of polyvinyl alcohol-gelatin hydrogel membranes for biomedical applications, AAPS PharmSciTech 8 (2007) E142−E146, https://doi.org/10.1208/pt080121.

[35] N.A. Peppas, S.R. Stauffer, Reinforced uncrosslinked poly (vinyl alcohol) gels produced by cyclic freezing-thawing processes: a short review, J. Contr. Release 16 (1991) 305−310, https://doi.org/10.1016/0168-3659(91)90007-Z.

[36] S.R. Stauffer, N.A. Peppas, Poly(vinyl alcohol) hydrogels prepared by freezing-thawing cyclic processing, Polymer (Guildf) 33 (1992) 3932−3936, https://doi.org/10.1016/0032-3861(92)90385-A.

[37] C.M. Hassan, N.A. Peppas, Cellular PVA hydrogels produced by freeze/thawing, J. Appl. Polym. Sci. 76 (2000) 2075−2079, https://doi.org/10.1002/(SICI)1097-4628(20000628)76:14<2075::AID-APP11>3.0.CO;2-V.

[38] C.M. Hassan, N.A. Peppas, Structure and morphology of freeze/thawed PVA hydrogels, Macromolecules 33 (2000) 2472−2479, https://doi.org/10.1021/ma9907587.

[39] C.M. Hassan, J.H. Ward, N.A. Peppas, Modeling of crystal dissolution of poly(vinyl alcohol) gels produced by freezing/thawing processes, Polymer (Guildf) 41 (2000) 6729−6739, https://doi.org/10.1016/S0032-3861(00)00031-8.

[40] C. Zhao, X. Lu, Q. Hu, S. Liu, S. Guan, PVA/PEG hybrid hydrogels prepared by freeze-thawing and high energy electron beam irradiation, Chem. Res. Chin. Univ. 33 (2017) 995−999, https://doi.org/10.1007/s40242-017-7107-9.

[41] A.S. Ahmed, U.K. Mandal, M. Taher, D. Susanti, J.M. Jaffri, PVA-PEG physically cross-linked hydrogel film as a wound dressing: experimental design and optimization, Pharmaceut. Dev. Technol. 23 (2018) 751−760, https://doi.org/10.1080/10837450.2017.1295067.

[42] L. Zhang, Z. Wang, M. Xu, B. Duan, Y. Chen, M. He, Y. Zhao, Y. Cao, Construction of chitin/PVA composite hydrogels with jellyfish gel-like structure and their biocompatibility, Biomacromolecules 15 (2014) 3358−3365, https://doi.org/10.1021/bm500827q.

[43] X. Yang, Z. Zhu, Q. Liu, X. Chen, M. Ma, Effects of PVA, agar contents, and irradiation doses on properties of PVA/ws-chitosan/glycerol hydrogels made by γ-irradiation followed by freeze-thawing, Radiat. Phys. Chem. 77 (2008) 954−960, https://doi.org/10.1016/j.radphyschem.2008.02.011.

[44] S. Shi, X. Peng, T. Liu, Y.N. Chen, C. He, H. Wang, Facile preparation of hydrogen-bonded supramolecular polyvinyl alcohol–glycerol gels with excellent thermoplasticity and mechanical properties, Polymer (Guildf) 111 (2017) 168−176, https://doi.org/10.1016/j.polymer.2017.01.051.

[45] S. Peng, S. Liu, Y. Sun, N. Xiang, X. Jiang, L. Hou, Facile preparation and characterization of poly(vinyl alcohol)-NaCl-glycerol supramolecular hydrogel electrolyte, Eur. Polym. J. 106 (2018) 206−213, https://doi.org/10.1016/j.eurpolymj.2018.07.024.

[46] G.L. Li, J.T. Wu, Y.H. Xia, Q.G. He, H.G. Jin, Review of semi-dry electrodes for EEG recording, J. Neural. Eng. 17 (2020), https://doi.org/10.1088/1741-2552/abbd50.

[47] G. Li, S. Wang, Y.Y. Duan, Towards conductive-gel-free electrodes: understanding the wet electrode, semi-dry electrode and dry electrode-skin interface impedance using electrochemical impedance spectroscopy fitting, Sensor. Actuator. B Chem 277 (20 December 2018) 250−260, https://doi.org/10.1016/j.snb.2018.08.155.

[48] M.A. Lopez-Gordo, D. Sanchez Morillo, F. Pelayo Valle, Dry EEG electrodes, Sensors (Switzerland) 14 (2014) 12847−12870, https://doi.org/10.3390/s140712847.

[49] B.J. Polk, A. Stelzenmuller, G. Mijares, W. MacCrehan, M. Gaitan, Ag/AgCl microelectrodes with improved stability for microfluidics, Sensor. Actuator. B Chem. 114 (2006) 239−247, https://doi.org/10.1016/j.snb.2005.03.121.

[50] M.J.G. Lito, M.F. Camões, Meeting the requirements of the silver/silver chloride reference electrode, J. Solut. Chem. 38 (2009) 1471−1482, https://doi.org/10.1007/s10953-009-9462-8.